Glass-wool study of laser-induced spin currents en route to hyperpolarized Cs salt

Kiyoshi Ishikawa
Graduate School of Material Science, University of Hyogo, Ako-gun, Hyogo 678-1297, Japan
(Received 13 May 2011; published 7 July 2011)

The nuclear spin polarization of optically pumped Cs atoms flows to the surface of Cs hydride in a vapor cell. A fine glass wool lightly coated with the salt helps greatly increase the surface area in contact with the pumped atoms and enhance the spin polarization of the salt nuclei. Even though the glass wool randomly scatters the pump light, the atomic vapor can be polarized with unpolarized light in a magnetic field. The measured enhancement in the salt enables study of the polarizations of light and atomic nuclei very near the salt surface.

DOI: 10.1103/PhysRevA.84.013403 PACS number(s): 32.80.Xx, 32.30.Dx, 34.35.+a, 76.60.−k

I. INTRODUCTION

One of the recent developments for overcoming small detection efficiency in conventional nuclear magnetic resonance (NMR) is hyperpolarization of materials; namely, the nuclear spin polarization can be much higher than the one attained in the thermal equilibrium. One example is the noble gas polarized by spin-exchange optical pumping [1–5]. The source of spin polarization—the laser-polarized alkali-metal atom—moves around, transferring the angular momentum to targets efficiently with the spin-exchange interaction between electrons and nuclei of atoms. Another example is the dynamic nuclear polarization of a LiF crystal at low temperature [6]. Since the spin polarization diffuses throughout the crystal by a nuclear dipole interaction, we need to design carefully the rates of spin decay and buildup caused by the source—paramagnetic electrons fixed in a crystal [7]. Much anticipated is the hyperpolarization of a solid in a universal way such that a current of spin polarization of atoms or electrons is externally injected into a solid. This experiment surely advances the study on spin dynamics at the interface as well as in the gas and solid phases.

The nuclei in alkali-metal salts were polarized by optical pumping of atomic vapor [8]. The polarized Cs atoms transported spin angular momentum to the salt. The nuclear spin current was found to be a primary source of salt polarization [9]. The Cs NMR signal was four times larger than the value in the thermal equilibrium observed for solid CsH at 9.4 T, and 17 times larger at 2.7 T. Although the signal was also enhanced at 0.56 T, the thermal signal was too small to estimate the enhancement factor. This paper reports the 80-fold enhancement at the low field. The advanced technique uses quartz-glass wool for transferring angular momentum to salt in a vapor cell. The Cs hydride is formed on fine glass fibers with a considerable increase of surface area. The atomic nuclei can be polarized although the glass wool randomly scatters the pump light. The polarized atoms then have many opportunities for spin transfer to the salt. The enhanced signal is large enough to measure the nuclear spin current in the glass-wool cells.

II. EXPERIMENT

The quartz-glass wool (impurities < 50 ppm, Tosoh Quartz Co.) was put into the glass cell without any additional treatments. The diameter of glass fibers mostly ranged from 4 to 9 μm. Cs metal reacts *in situ* with hydrogen gas, and the hydride, CsH and CsD, formed on the fiber must have large surface area. The salt cells were manufactured as described previously [8,9]. The Cs NMR signal of hydride was measured at 0.56 T with the setup shown in Fig. 1. Since the metal signal was in far off-resonance, we detected only the Cs nuclei in the salt. Applying a single radio-frequency (rf) pulse, we recorded the free induction decay, averaged as many times as needed, and analyzed the Fourier transform. The resistive heater outside the magnet conductively heated the glass cell. Additionally, the laser increased the cell temperature. Due to the temperature gradient generated in this way, Cs metal moved away from the detection range of the NMR coil into the stem of the glass cell. The loss of rf field caused by the metal was then negligible, and the quality of the tuning circuit was high enough for solid NMR. It was more essential to the spin transfer that the uncovered hydride was exposed to the polarized vapor. Since the metal nuclei are easily unpolarized [10], the metal film would prevent the spin polarization of vapor from transferring to salt.

The pump laser was tuned to the D_2 line ($6s\,^2S_{1/2} \rightarrow 6p\,^2P_{3/2}$) of Cs atoms, and the beam perpendicular to magnetic field was linearly polarized for π or σ pumping. Because the electron Zeeman splitting is close to the hyperfine splitting of the ground state, the sublevel $|m_S,m_I\rangle = |I\,m_I\rangle \otimes |S\,m_S\rangle$ is greatly mixed with $|m'_S,m'_I\rangle$, where $m_S + m_I = m'_S + m'_I$. The atomic nuclei are optically polarized through this state mixing, while the spin polarization due to collisions is negligible at the low fields. As shown in the absorption cross section in Fig. 2(a), π light is strongly absorbed at the small detuning, σ light is competitively absorbed with π light at ± 5 GHz, and the resonant absorption of σ light is two orders of magnitude larger than π light at ± 25 GHz. The absorption length is 0.5 mm for the maximum cross section and the number density of Cs atoms is $[\mathrm{Cs}] = 7.8 \times 10^{12}$ cm^{-3} at 90 °C.

In spite of uniform density [Cs], a spatial gradient of spin polarization is generated because atoms are unpolarized at the walls, which is well justified by the experiments [9,11]. The nuclear polarization of atoms desorbing from the walls is negligibly small. Therefore, optical pumping causes the diffusion spin currents to the wall, the amplitude of which depends on laser frequency and polarization as well as buffer-gas pressure. The nuclear spin current along the slope is $J_I = -[\mathrm{Cs}]D\partial\langle I_z\rangle/\partial r$, where r is the radial coordinate of the cylindrical cell and D is the diffusion coefficient of Cs

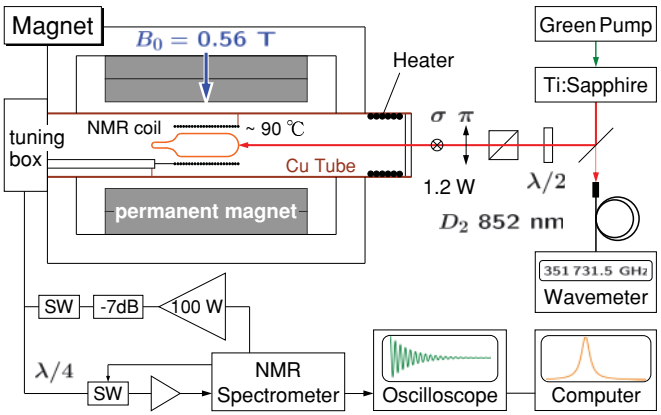

FIG. 1. (Color online) Schema for optical pumping of Cs atoms and Cs NMR of salt. A permanent magnet produces the field 0.56 T, and the homogeneity is 15 ppm for a cylindrical cell of inner diameter 8 mm. The cell is heated with a copper tube and an electric heater and irradiated with π or σ light passing through a half-wave ($\lambda/2$) plate.

atoms [8]. Assuming that the optical pumping beam uniformly fills the entire volume of the cylindrical cell which contains no glass wool [9], we numerically solved the evolution equation of the density matrix [12,13]. As shown in Fig. 2(b), the spin current at the sidewall is calculated for each light polarization to study light polarization mixing by glass wool. Since many optical transitions induce various combinations of currents, D_2 pumping is suitable to study laser-induced spin current. The accumulation of angular momentum is proportional to

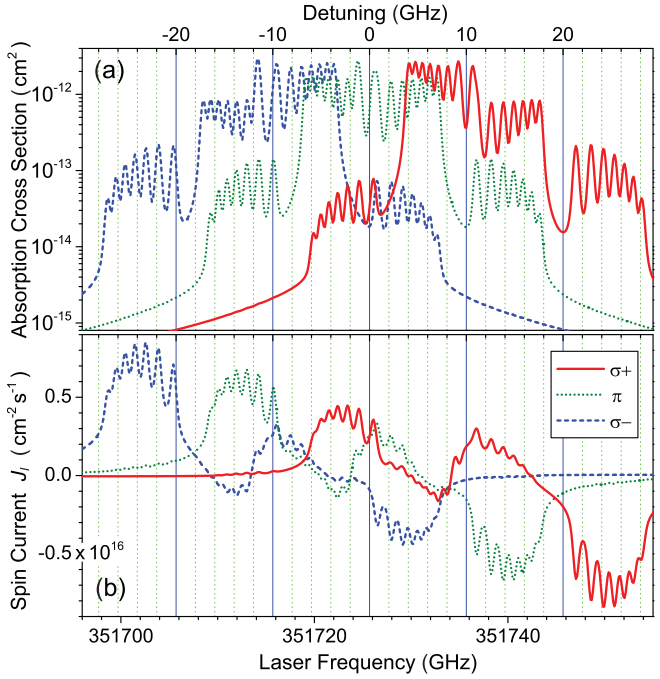

FIG. 2. (Color online) (a) Absorption cross section and (b) nuclear spin current calculated for each light polarization at the D_2 line, 0.56 T, and 1.5 kPa N_2. We assumed uniform pumping at 1 W/cm^2 and the boundary condition, $\langle S_z \rangle = \langle I_z \rangle = 0$, at the sidewall ($r = 4$ mm) of the cylindrical cell. The spin-exchange interaction between Cs atoms was neglected.

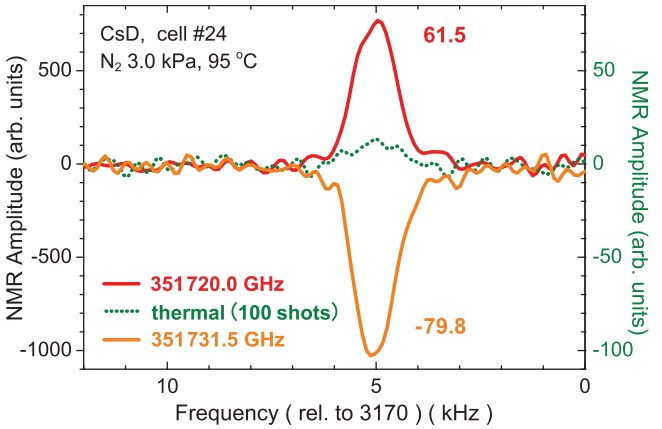

FIG. 3. (Color online) Cs NMR signal optically enhanced by σ pumping. CsD salt was formed on glass wool and filled with Cs metal and 3.0 kPa N_2 gas. The positive (red, enhancement 61.5) and negative (orange, -79.8) signals were recorded without averaging, respectively, for the laser frequencies 351 720.0 and 351 731.5 GHz. Thermal signal scaled by the right-hand vertical axis (dotted green curve) was averaged a hundred times with the repetition interval of 10 min.

the inflow of spin current and the spin relaxation time in the solid. Therefore, we compare the spin current simulated for the cylindrical cell to the observed NMR enhancement.

The NMR signals were detectable by a single shot only with the glass wool and optical pumping, as shown in Fig. 3. An rf pulse was applied after the accumulation time was sufficiently larger than the spin relaxation time in the salt. The area of the resonance peak, A, is proportional to the spin polarization P of Cs nuclei. From the enhancement ($A/A_{\rm th} = -79.8$) and the polarization in the thermal equilibrium at 95 °C ($P_{\rm th} = 6.21 \times 10^{-7}$), the spin polarization was an average of $P = -5.0 \times 10^{-5}$. When the salt is thicker than the spin diffusion length ($\lesssim$100 nm) [7], the polarization is higher at the surface than at the center of the crystallites. The enhanced signal was mostly from the salt on the fibers, although the thermal signal was from all the salt, including the thick layer on the sidewall. We are able to increase the average of nuclear polarization when a salt consists only of film.

III. OPTICAL NMR ENHANCEMENT

In this section, we present the laser frequency dependence of NMR area A for several glass cells. As shown in Fig. 4(a), the cylindrical cells with *no* glass wool exhibited double positive peaks at -8 and -5 GHz, and negative enhancement at $+5$ GHz. By comparing with the curves of spin currents, the enhancement was found to be primarily due to the nuclear spin current [9]. The optical transition corresponds roughly to the high-field transition, $|m_S, m_I\rangle \rightarrow |m_J, m_I'\rangle$: ($\sigma_-$ light) $|-1/2, m_I\rangle \rightarrow |-3/2, m_I\rangle$ and (σ_+) $|1/2, m_I\rangle \rightarrow |1/2, m_I + 1\rangle$ for a positive peak, (σ_-) $|-1/2, m_I\rangle \rightarrow |-1/2, m_I - 1\rangle$ and (σ_+) $|1/2, m_I\rangle \rightarrow |3/2, m_I\rangle$ for a negative peak. Since the enhancement was at most $A/A_{\rm th} \approx 10$, it took a long time for averaging, and then the measurement was limited to the small laser detuning. With the glass wool, the NMR signal was greatly enhanced

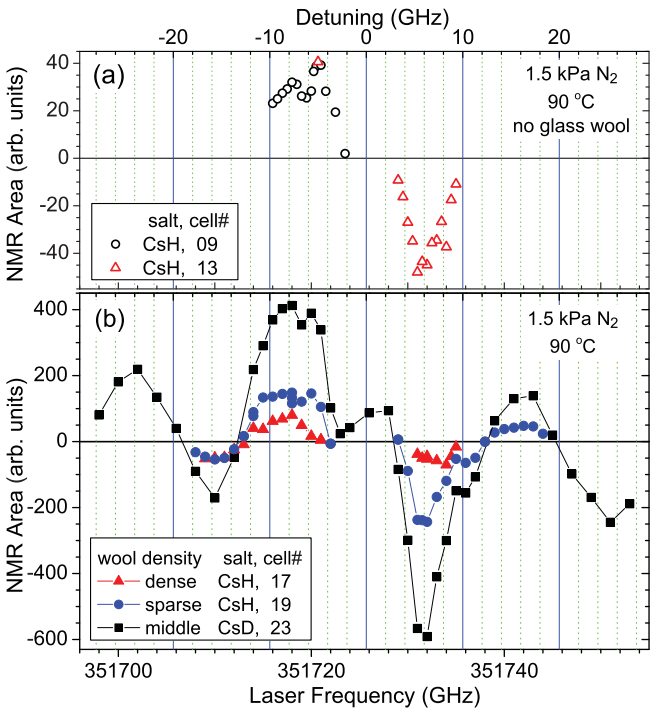

FIG. 4. (Color online) Laser-frequency dependence of the NMR area enhanced by σ pumping at 1.5 kPa N_2. The vertical axis is in arbitrary units but can be compared with the other plots in this paper. Radio-frequency pulses of the tipping angle $\pi/3$ were applied at the repetition interval 100 s. (a) CsH at the sidewall of two cylindrical cells (○, △) with no glass wool. The signal was averaged 70 times for each point. (b) CsH and CsD formed on the glass fibers. The apparent density of the glass wool was (▲) dense, (■) medium, and (●) sparse, judged visually.

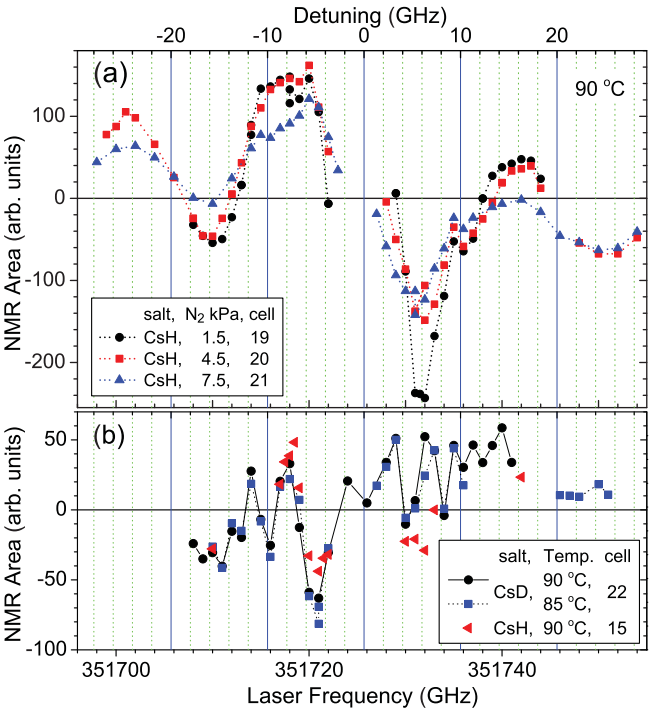

FIG. 5. (Color online) Pressure dependence of NMR enhancement for σ pumping in the glass-wool cells. (a) CsH filled with N_2 gas at (●) 1.5 kPa, (■) 4.5 kPa, and (▲) 7.5 kPa. (b) CsD in vacuum (●, 90 °C; ■, 85 °C) and CsH with the original pressure 4.0 kPa of H_2 gas (◀).

by optical pumping and was able to measure across the D_2 line, as shown in Fig. 4(b). The long-term averaging was unnecessary and only a few signals were averaged to reduce amplitude scattering. The positive enhancement near -5 GHz still presents the double peaks. Except for the amplitude, the enhancement curves for the cells with or without glass wool resemble each other. Therefore, the spin current calculated for a cylindrical cell is useful to study the enhancement for glass-wool cells, although the bounded space was much smaller than the cell's dimension.

In a cylindrical cell with a buffer gas but no glass wool, most atoms are pumped by the intense light and the atomic vapor is almost transparent. The atoms are, however, unpolarized at the surface as described above. The pump beam parallel to the cell axis experiences strong absorption all along the sidewall. As a result, the pump light is weak near the wall. On the other hand, the surface of the fiber is randomly directed, and the intense light can pump the atoms confined in the glass wool. The fiber glass scatters but does not absorb the light. Therefore, the glass wool enables optical pumping of the atoms very near the surface, and the salt on the fiber was efficiently exposed to the *polarized* atoms.

Figure 4(b) shows the NMR enhancement for various densities of glass wool. When the wool is too dense for the pump light to percolate properly, the salt nuclei are polarized only near the window, resulting in the enhanced signal (triangle) only twofold larger than that without the wool. For the sparse wool (circle), Cs atoms are polarized uniformly in the entire space of the cell, but the surface area of the salt is insufficient. Since the wool also scatters the pump light to take a long path, there should be an optimal density of wool for the spin transfer to salt via atomic vapor. The current optimal density is shown by squares. The achieved polarization is assumed independent of either H or D because the spin relaxation time of Cs nuclei was the same for both hydrides.

Figure 5(a) shows the enhancement as a function of the buffer-gas pressure. The nuclear spin polarization of atoms was mostly due to direct optical pumping dominated by quenching, with less contribution from hyperfine-shift pumping [9]. The current J_I is nearly constant for increasing pressure because the decrease of the coefficient D cancels the increase of the slope $\partial\langle I_z\rangle/\partial r$. Therefore, the pressure dependence of the enhancement was small. As shown in Fig. 5(b), the NMR area varied from point to point for a vacuum glass-wool cell. The sharp profile was different from the buffer-gas cells and, more importantly, different from the vacuum cells with no glass wool [9]. There should be something intrinsic to the vacuum and glass-wool cell, such as that the excited atoms move freely in a confined space and transfer the polarization to the salt [14], although it is still an open question.

Until this point, we used the glass cells sealed after the chemical reaction of Cs metal with hydrogen gas. Although wet tissues prevented the cells from overheating via torch, it might be possible to change the surface of the hydrides during the sealing-off procedure. Expecting the reaction after

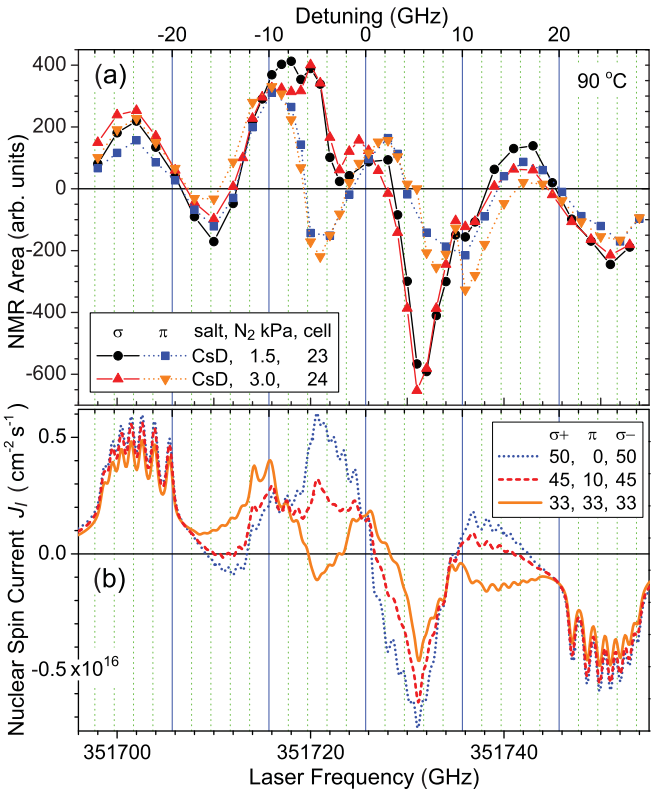

FIG. 6. (Color online) (a) Light-polarization dependence of enhancement for CsD filled with 1.5 kPa and 3.0 kPa N_2 gas. NMR area was measured with (●, ▲) σ light and (■, ▼) π light. (b) Nuclear spin current simulated for σ (dotted blue) and mixed (dashed red, solid orange) polarizations in a cylindrical cell with no glass wool. The relative power of each polarization is shown as a percentage. The current by polarization mixing is not simply a sum of currents by each component of light polarization.

sealing, the glass cell was filled with H_2 gas at the original pressure of 4 kPa and left at room temperature for a month. It was long enough because the existing hydride can be the crystalline nuclei. In Fig. 5(b), we find that the enhancement is consistent with the vacuum cell. H_2 molecules had reacted with the excess Cs metal, resulting in vacuum. Because of no significant change in NMR area, the spin-transfer mechanism was insensitive to the fine distinction between the manufacturing processes. For the respective cells with or without the buffer gas, the signals were still enhanced at the initial amplitude after the continuous laser irradiation at 1 W for several consecutive days. In spite of a dissociative salt, the hydride unexpectedly exhibited toughness at 90 °C.

IV. LIGHT POLARIZATION CONVERSION

The pump-polarization dependence of the enhancement is shown in Fig. 6(a). Two independent cells presented similar spectral shapes for σ and π lights, respectively, and the different details depending on the individual cell. One example is the relative amplitude of double peaks for σ pumping. Taking into account that peaks are due to σ_- pumping at -8 GHz and σ_+ pumping at -5 GHz, linearly polarized σ light changed to different combinations of σ_+ and σ_- light in these cells. It is

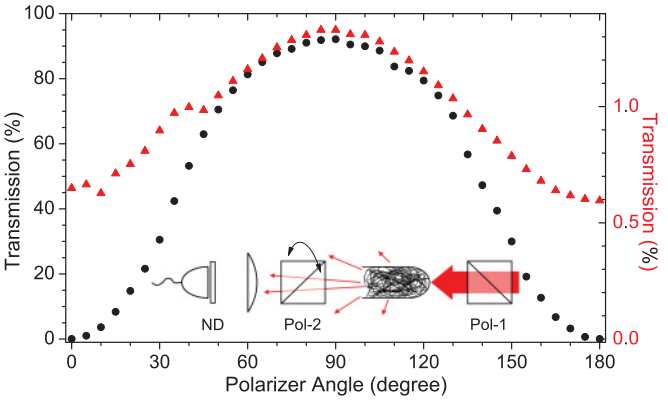

FIG. 7. (Color online) Light transmission through a test cell with (▲, right vertical scale) and without (●, left vertical scale) the glass wool. Horizontal axis is the rotation angle of the second polarizer. The inset shows the optics arrangement.

also noted that the signal has a similar amplitude at ± 25 GHz for σ and π lights, although J_I for pure polarization is much different for σ and π lights, as shown in Fig. 2(b).

This observation suggests that the polarization of the incident beam was converted to the other polarization in the cell. Since crystallites and glass fibers were visually white in color, they were larger than the wavelength of visible light [15] and geometric optics is useful to study light scattering. The fibers were randomly directed, and the light polarization and propagation were randomized through the multiple reflections and refractions [16]. The absorption in quartz glass is negligible at the laser wavelength. It seems like the diffusion motion of photons is forced by the artificial material with a loss due to the absorption by atoms. Accordingly, the optical path length can be larger than the cell dimension. In the case of sending π light, the pump light becomes mixed with σ light as it propagates in the glass wool. When σ light is absorbed, the pump light attains again the mixed polarization from the remaining π light. The spin current induced by σ light is dominant whether the original beam is σ or π light. We compare the observed enhancement in Fig. 6(a) with the spin current in Fig. 2(b) by taking into account the absorption in Fig. 2(a). Since the absorption at ± 25 GHz is larger for σ light than π light, the spin current induced by σ light is dominant no matter the original polarization. In the same way, the spin current by π light is dominant at the small detuning. On the other hand, because the absorption at ± 5 GHz is comparable for both polarizations, the pump light induces the spin current primarily according to the polarization of incident beam. The spin current shown in Fig. 6(b) is a simulation at various ratios of polarization mixing, but in a real cell, the ratio varies as the light is multiply scattered in the glass wool.

Figure 7 shows the measurement of light-polarization mixing by the glass wool. The curved window of a test cell was similar to cells used in the pumping experiment, but the output window was removed to measure the light polarization. The density of glass wool was equal visually to that in the cells for Fig. 6. The incident beam was linearly polarized at the D_2 line. The polarization remained linear through the window. With the glass wool, the laser light was scattered to a wide spread of direction and the forward-scattered light was

poorly polarized. Since the widely scattered light can be more randomly polarized, we expect that the pump polarization was mixed in the real cells to be strongly absorbed by atoms.

In contrast to mixing of pump light with the emission of atoms in the previous work [9], the glass wool greatly facilitated polarization mixing, resulting in significant enhancement of the Cs NMR signal. We found, however, no enhancement of ^{2}H NMR for CsD in the identical glass-wool cell. We expected the nuclear dipolar interaction for spin transfer from vapor to solid. The frequency difference between 3175 kHz (^{133}Cs) and 3716 kHz (^{2}H) is too large for them to couple with each other. Thermal mixing at low fields is hopefully suitable for the spin polarization of deuterons.

V. SUMMARY

The quartz-glass wool worked to considerably enhance the nuclear spin polarization in the Cs hydride by optical pumping of Cs vapor. The average nuclear polarization reached 80 times the thermal equilibrium at 0.56 T. We should be able to measure true enhancement once the thermal signal of salt on the glass fibers is detected separately from thick salt on the sidewall. Due to the Zeeman splitting, the absorption cross section depends on light polarization, and unpolarized light was then available for polarizing Cs vapor. The glass wool functioned in several ways: (i) the large surface area of salt was in contact with the optically polarized atomic vapor, (ii) the thin film better matched the spin diffusion length in the salt, (iii) the Cs atoms were optically polarized even near the salt because of the random direction of the surface normal, (iv) the laser polarization was adaptively converted to strong absorption by random scattering, and (v) the effective path length of the pumping light was extended via multiple scattering by glass wool. By these technical advances, we reconfirmed that the nuclear spin polarization of salt was mostly due to the nuclear spin current induced by optical pumping. Conversely, we were able to measure the nuclear spin current in the random scattering medium by monitoring the NMR signal of salt.

ACKNOWLEDGMENTS

The author would like to thank W. Happer, Y.-Y. Jau, B. Patton, and B. A. Olsen for collaboration at an early stage of the project and the recent discussion and comments, and R. Inoue and Y. Izutsu for manufacturing an NMR magnet. This work was supported by the Grant-in-Aid for Scientific Research of JSPS, Japan.

[1] T. G. Walker and W. Happer, Rev. Mod. Phys. **69**, 629 (1997).
[2] D. Raftery, H. Long, T. Meersmann, P. J. Grandinetti, L. Reven, and A. Pines, Phys. Rev. Lett. **66**, 584 (1991).
[3] B. Driehuys, G. D. Cates, and W. Happer, Phys. Rev. Lett. **74**, 4943 (1995).
[4] T. Rõõm, S. Appelt, R. Seydoux, E. L. Hahn, and A. Pines, Phys. Rev. B **55**, 11604 (1997).
[5] K. Ishikawa, T. Yamamoto, and Y. Takagi, J. Magn. Reson. **179**, 234 (2006).
[6] J. Ball, Nucl. Instrum. Methods Phys. Res., Sect. A **526**, 7 (2004).
[7] A. Abragam, *Principles of Nuclear Magnetism* (Clarendon Press, Oxford, 1961).
[8] K. Ishikawa, B. Patton, Y. Y. Jau, and W. Happer, Phys. Rev. Lett. **98**, 183004 (2007).
[9] K. Ishikawa, B. Patton, B. A. Olsen, Y.-Y. Jau, and W. Happer, Phys. Rev. A **83**, 063410 (2011).
[10] J. Korringa, Physica **16**, 601 (1950).
[11] B. A. Olsen, Ph.D. thesis, Princeton University, 2011.
[12] S. Appelt, A. B.-A. Baranga, C. J. Erickson, M. V. Romalis, A. R. Young, and W. Happer, Phys. Rev. A **58**, 1412 (1998).
[13] W. Happer, Y.-Y. Jau, and T. G. Walker, *Optically Pumped Atoms* (Wiley-VCH, Weinheim, 2010).
[14] D. Sarkisyan, D. Bloch, A. Papoyan, and M. Ducloy, Opt. Commun. **200**, 201 (2001).
[15] M. Born and E. Wolf, *Principles of Optics* (Cambridge University Press, New York, 1999).
[16] M. C. W. van Rossum and T. M. Nieuwenhuizen, Rev. Mod. Phys. **71**, 313 (1999).